

Retention of the Goss orientation between microbands during cold rolling of an Fe3%Si single crystal

Dorothee Dorner, Stefan Zaeferrer *, Dierk Raabe

Max-Planck-Institut für Eisenforschung, 40237 Düsseldorf, Germany

Received 13 October 2005; received in revised form 13 November 2006; accepted 18 November 2006

Available online 14 February 2007

Abstract

An FeSi single crystal with an initial $\{110\}\langle 001\rangle$ orientation, also referred to as Goss orientation, was cold rolled up to a thickness reduction of 89%. Most of the crystal volume rotated into the two symmetrical $\{111\}\langle 112\rangle$ orientations. However, a weak Goss component remained in the highly strained material, even though the Goss orientation is mechanically unstable under plane strain loading. Two types of Goss-oriented regions were discernable in the material subjected to 89% reduction. It appeared that these two types of Goss regions have different origins. Goss grains that were found aligned in shear bands form during straining. A second type of Goss region was found between microbands where the initial Goss orientation was retained.

© 2007 Acta Materialia Inc. Published by Elsevier Ltd. All rights reserved.

Keywords: Silicon steel; Goss orientation; Cold rolling; Microband; Shear band

1. Introduction

Silicon steel is a soft magnetic material that is used in electrical power transformers, motors and generators. It has a high silicon content of about 3.2 mass%, which increases the electrical resistivity of iron and, therefore, reduces eddy current losses. Grain-oriented silicon steel that is used for non-rotating applications, i.e. transformers, is characterised by a strong preferred crystallographic orientation. In iron the easiest directions of magnetisation are the $\langle 001\rangle$ crystal directions. In grain-oriented silicon steel the Goss orientation, i.e. the $\{110\}\langle 001\rangle$ orientation¹, is technologically realised to minimise magnetic losses in electrical transformers.

The strong Goss texture of grain-oriented silicon steel is the result of a complex processing scheme, i.e. of a long

microstructural and textural inheritance chain. The origin of the evolution of the final Goss orientation is in the hot rolling stage, where the Goss orientation develops below the sheet surface due to shear deformation [1–4]. The particular importance of this Goss-containing subsurface layer was demonstrated by experiments in which the removal of this layer resulted in incomplete secondary recrystallisation [5,1,6]. In the cold rolled material, the fraction of the Goss orientation, considering a misorientation of up to 15°, is about 1% as measured using electron backscatter diffraction (EBSD) [7]. This means that the Goss component is too weak to be detected by X-ray diffraction, as used in earlier studies [e.g. 8,1,9]. In the subsequent primary annealing step, the material recrystallises and the Goss component slightly increases. In the final secondary high-temperature annealing process, normal grain growth is inhibited by particles. However, some of the Goss grains that are present in the recrystallised material grow abnormally. This gives rise to a sharp Goss texture with an average misorientation from the exact Goss orientation of about 3–7°. The exact mechanisms of inheritance of the Goss orientation through

* Corresponding author.

E-mail address: s.zaeferrer@mpie.de (S. Zaeferrer).

¹ $\{hkl\}$: Crystallographic plane that is parallel to the sheet plane $\langle uvw\rangle$: crystallographic direction that is parallel to the rolling direction.

the process chain and details of abnormal Goss grain growth in the secondary annealing stage are still unclear [10].

The investigation of the microstructural evolution of the Goss orientation from the hot rolling stage to the final secondary recrystallisation in the industrially processed material is difficult, since Goss grains are very rare both in the cold rolled and the primary recrystallised state. However, in an early study Dunn [11] observed that, after deformation and primary recrystallisation of an initially Goss-oriented single crystal, the volume fraction of Goss grains is higher than in the industrially processed polycrystalline material. Moreover, Mishra et al. [1] pointed out that the large Goss grains that are present in the subsurface layer of hot rolled silicon steel (Fig. 1) and which are essential for the development of the final Goss texture, qualitatively behave like Goss-oriented single crystals. Therefore, in this study a Goss-oriented single crystal was used as the starting material for the cold rolling and annealing experiments (Fig. 1). Such model experiments allow a detailed investigation of Goss grains in the deformed state and therefore might lead to an improved understanding of the incipient state of primary recrystallisation. Furthermore, Goss grains in the primary recrystallised state, which provide the nuclei for secondary recrystallisation, specifically for abnormal Goss grain growth, can be characterised in detail. One particular question in this context is whether these grains have particular properties that allow them to grow abnormally.

This publication exclusively focuses on the evolution of the microstructure and microtexture of the initially Goss-oriented FeSi single crystal during cold rolling. The results of the investigations on the primary recrystallised material will be presented in a forthcoming study. A detailed investigation of the microstructure evolution during cold rolling, with the aid of high-resolution EBSD, revealed that two types of Goss-oriented regions were present in the deformed material. These two types were related to either shear bands or microbands. These new findings particularly raised the following questions: (1) How is some fraction of the starting single crystal Goss orientation retained

during cold rolling, even though it is mechanically unstable in body-centred cubic (bcc) metals upon plane strain deformation [12,13]? Or does it disappear and reform during rolling deformation? (2) What are the roles of shear bands and microbands during rolling deformation, in particular for the stabilisation of the Goss orientation?

2. Experimental procedure

The starting material for this study was an industrially hot rolled silicon steel strip with 3.24 mass% Si and MnS as an inhibitor, which is employed for the production of conventional grain-oriented (CGO) electrical steel. This material was used to grow a single crystal with $\{110\}$ $\langle 001 \rangle$ orientation using the Bridgman method. First, the sample was connected to a Goss-oriented seed crystal. Then the sample and a part of the seed crystal were melted and subsequently solidified starting from the seed crystal. This resulted in a single crystal sample with the orientation of the seed crystal (Fig. 2). The as-grown single crystal was almost perfect, containing only a very small number of low-angle grain boundaries with misorientations of about 1° . The single crystal was machined to a thickness of 2.20 mm, which is about the thickness of a industrial hot rolled strip, a width of 21 mm and a length of about 55 mm. This strip was cold rolled without lubrication in a laboratory rolling mill with a roll diameter of 105 mm, a rolling velocity of 10 m/min and a load of 120 kN. In 14 passes the sample was rolled to a thickness of 0.25 mm corresponding to a total engineering thickness reduction of $\varepsilon = 89\%$ (true logarithmic strain of $\varphi = 2.2$).

The texture and microstructure of the deformed samples were investigated using electron diffraction techniques both in a scanning electron microscope (SEM) and in a transmission electron microscope (TEM). EBSD measurements were carried out using a field emission gun SEM (JEOL JSM 6500F). The software OIM (EDAX/TSL) was used to index the Kikuchi diagrams and for the evaluation of the orientation data. Microtexture measurements were also done by TEM and the Kikuchi patterns were indexed using the software Toca [14].

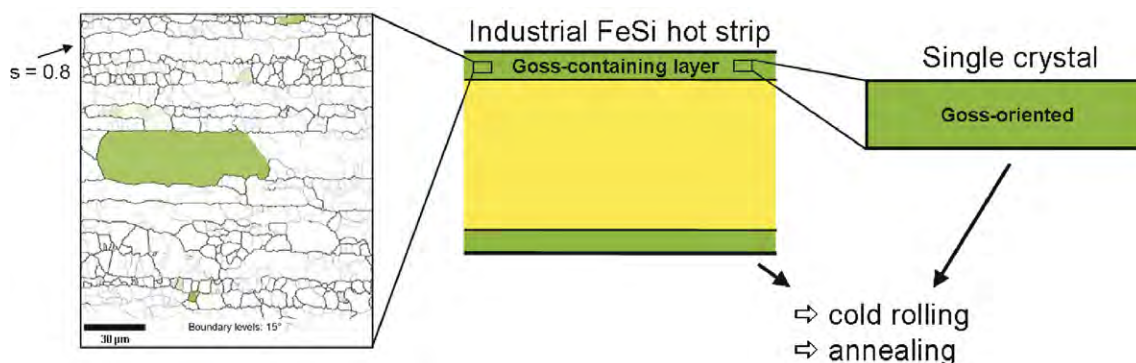


Fig. 1. Goss grain in an industrial FeSi hot strip (left) and the idea of the single crystal experiments (right).

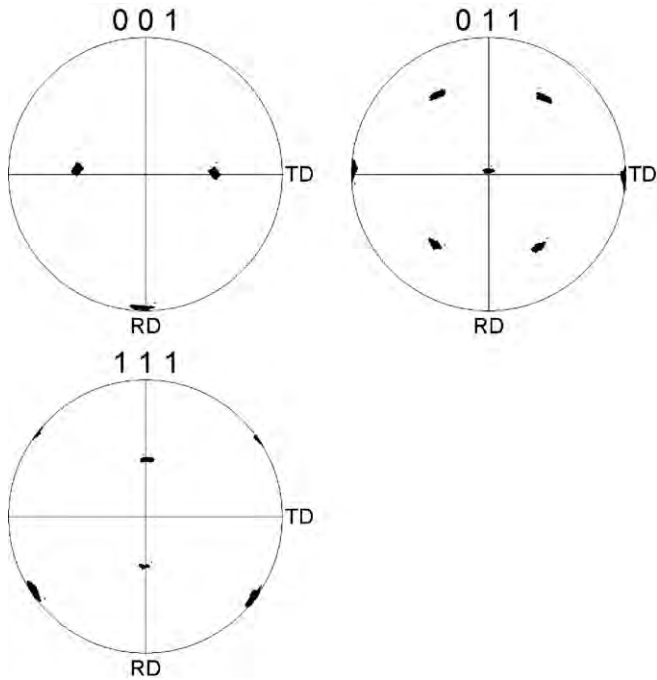


Fig. 2. Orientation of single crystal before cold rolling. Pole figures obtained from EBSD measurements.

3. Results

3.1. Texture and microstructure evolution during cold rolling

Both X-ray and EBSD data showed that in the course of cold rolling most of the initially Goss-oriented single crystal rotated in two opposing directions to the two symmetrically equivalent $\{111\}\langle 112 \rangle$ orientations. This rotation amounted to 35° around the $\langle 110 \rangle$ crystal direction, which is parallel to the transverse sheet direction (TD). In con-

trast to earlier studies using X-ray diffraction (e.g. [11]), not only the two strong $\{111\}\langle 112 \rangle$ texture components were observed (Fig. 3a), but the EBSD data revealed that even after highest deformation of 89% a weak Goss component was present (Fig. 3b).

The evolution of the microstructure and microtexture during cold rolling was studied by EBSD. At low thickness reductions, the spatial distribution of the Goss and the $\{111\}\langle 112 \rangle$ texture components was quite inhomogeneous throughout the deformed sheet (Fig. 4). However, in the 89% deformed material the texture in the sheet center and in the region close to the sheet surface were very similar. This indicated that there was no pronounced effect of shear stress due to friction at the sheet surface.

Characteristic microstructural features were microbands and at higher strain microscopic shear bands, which are described in more detail below. Furthermore, mechanical twinning (first order twins) occurred. The twinning planes of the $\{100\}\langle 011 \rangle$ -oriented twins were parallel to the transverse direction and inclined by about 10° to the rolling direction (RD). The volume of these deformation twins increased during deformation up to 61% thickness reduction and decreased at higher strain.

3.2. Occurrence of microbands and shear bands

EBSD and TEM investigations revealed that microbands frequently form during cold rolling of the Goss-oriented single crystal (Figs. 5 and 6). *Open microband* denotes a microstructural feature that is characterised by two straight, closely spaced dense dislocation walls enclosing a small elongated volume [15]. A *closed microband* is an elongated, straight dense dislocation wall that often occurs in groups of parallel bands. In this study the misorientation across a single wall was about 10° or higher and the sense of rotation was opposite on two successive walls (Fig. 7).

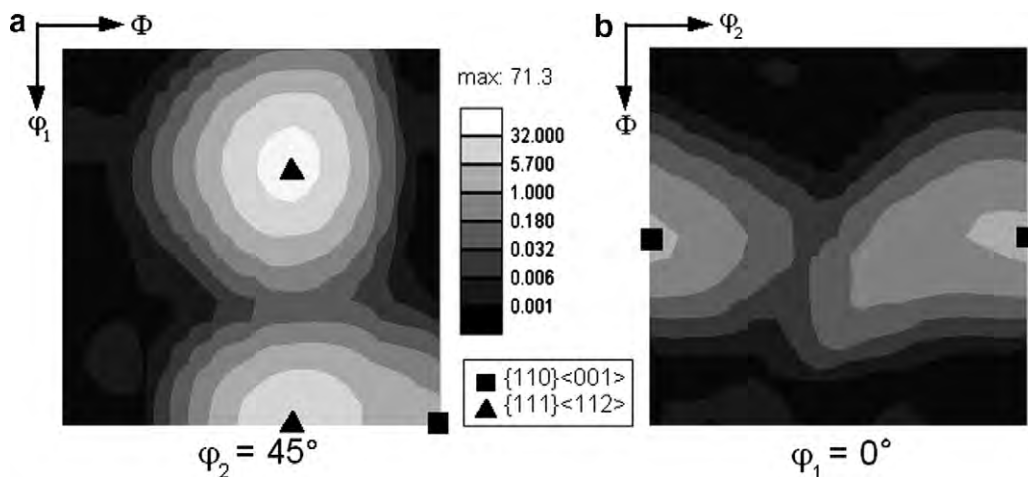


Fig. 3. Texture of the 89% deformed, initially Goss-oriented material. Orientation distribution function of EBSD data displayed in a $\varphi_2 = 45^\circ$ section (Bunge notation) (a) and a $\varphi_1 = 0^\circ$ section (b) through the Euler space. The texture components with the highest intensities are the two symmetrically equivalent $\{111\}\langle 112 \rangle$ components (a). In addition, a weak Goss component is observed, with a texture intensity of about 1 (b). Note that the texture intensity scale is logarithmic.

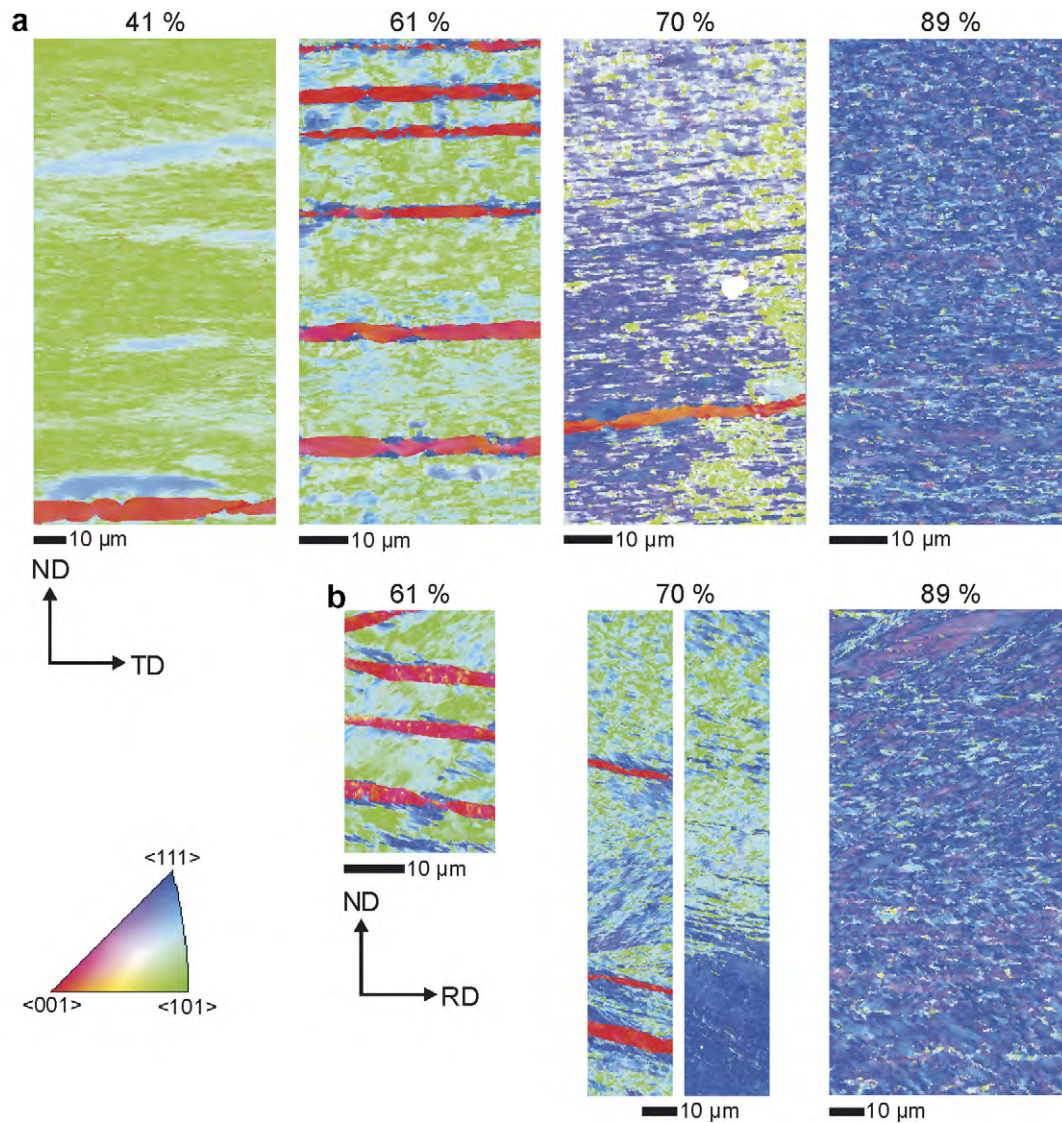


Fig. 4. Evolution of the microstructure during cold rolling of an initially Goss-oriented single crystal. Inverse pole figure maps for the normal sample direction as obtained by EBSD for samples with a thickness reduction of 41% ($\varphi = 0.5$), 61% ($\varphi = 1.0$), 70% ($\varphi = 1.2$) and 89% ($\varphi = 2.2$), respectively: (a) ND–TD sections; (b) ND–RD sections. ND: normal direction; RD: rolling direction; TD: transverse direction.

Therefore, the misorientation across a closed microband, which consists of two walls of opposite rotation, was very small. These observations were consistent with those of Chen et al. [15], although they observed a smaller misorientation. This difference might be attributed to the fact that they investigated less strained material.

At a strain of 55%, in some areas microbands started to form (Fig. 8), while in other areas they were already well developed (Fig. 6), indicating that deformation is inhomogeneous at lower strain. Fig. 8 shows an area with a microstructure characterised by two crossing sets of linear features with inclination with respect to the rolling direction of about 46° and 34° or less. Possibly this reflects an early stage of microband development, and presumably, during further deformation, these two sets would develop into the characteristic microstructure with parallel micro-

bands (Figs. 5 and 6). The parallel microbands were with about 22° less inclined (Fig. 6). Analysis of the orientation of the microbands with respect to the adjacent crystal orientation in both ND–TD sections and ND–RD sections (ND: normal direction) showed that the microband habit planes are close to $\{112\}$ crystal planes, but not related to $\{110\}$ planes. At 55% strain, many microbands comprised both open and closed parts (Fig. 7). At higher strain, the number of open microbands decreased and at the highest reduction of 89% all the microbands were closed. The inclination of the microbands decreased during straining until they were at the highest reduction roughly parallel to the rolling direction. At high strain of 89% thickness reduction, the microbands were still discernible in the deformed microstructure, but they occurred together with microscopic shear bands.

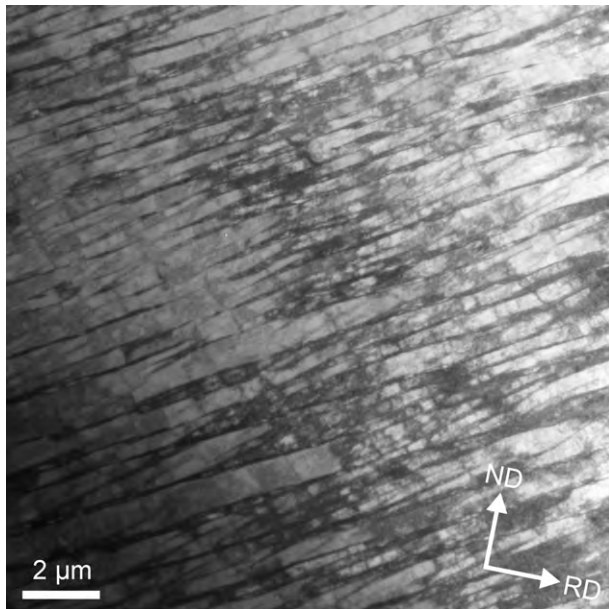


Fig. 5. Microbands in a 55% deformed, initially Goss-oriented single crystal. TEM bright field image.

Microscopic shear bands formed in cold rolled samples with thickness reductions of 77% ($\varphi = 1.5$) and higher [16]. They can be clearly recognized in EBSD pattern quality maps as linear features with a poor pattern quality (Figs. 9 and 10). The EBSD pattern quality generally becomes worse with increasing crystal lattice distortions due to a high dislocation density. The observed shear bands sheared the deformation twins, which developed at a lower strain. This observation was used to estimate the corresponding local shear strain to about 2. When viewed on ND–RD cross-sections, the shear bands were initially inclined by 29–36° to the rolling direction, with smaller inclination angles additionally occurring at higher strain [16]. The sense of inclination of the shear bands was dependent on the particular $\{111\}\langle 112\rangle$ orientation in which they developed (Fig. 9). The texture inside the shear bands consisted of the Goss orientation and the two symmetrical $\{111\}\langle 112\rangle$ components with varying intensities, but no additional orientations appeared [16]. These two observations, i.e. the correlation of shear band inclination with crystal orientation and the occurrence of only a limited number of crystal orientations inside the shear bands, revealed the crystallographic nature of the observed shear bands. Therefore, it can be assumed that the shear bands are so-called copper-type shear bands that develop due to geometrical softening as described by Dillamore et al. [17].

3.3. Evolution of the Goss orientation during cold rolling

In the 89% deformed samples, two types of Goss-oriented regions were discovered. Most of the Goss grains

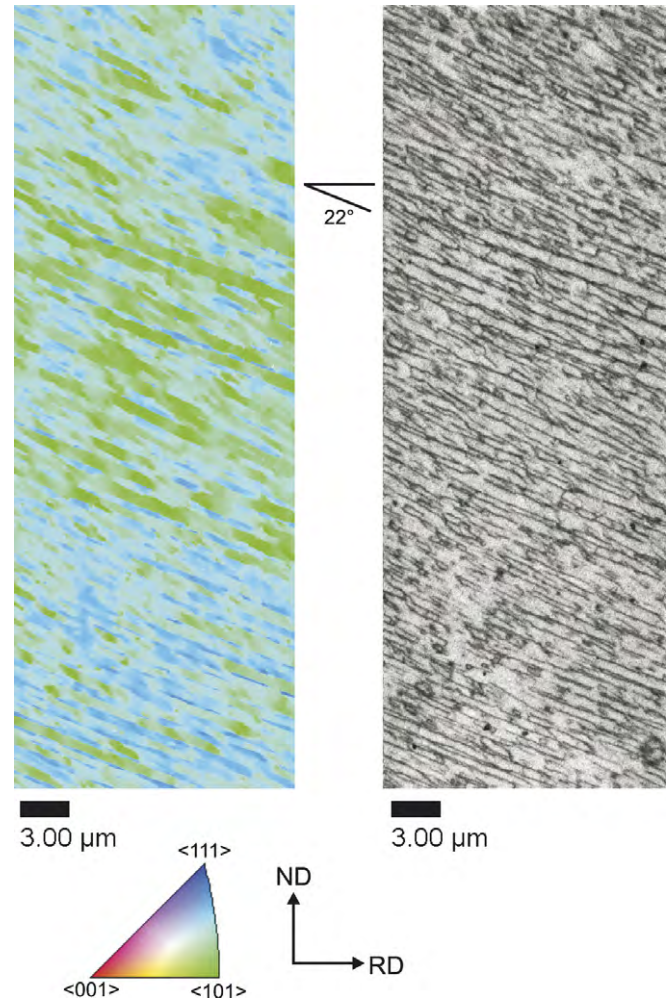


Fig. 6. Region with well-developed parallel microbands in a 55% deformed, initially Goss-oriented FeSi single crystal. The inclination of the microbands to RD is indicated. (a) Inverse pole figure map for the normal sample direction as obtained by EBSD. (b) EBSD pattern quality map showing microbands as linear features with low EBSD pattern qualities.

were situated inside the shear bands that developed in late stages of the rolling process (Fig. 10). The low EBSD pattern quality indicated that the stored strain energy of these Goss grains is high. Another type of Goss grains was found between microbands (Fig. 11), i.e. in regions with a high EBSD pattern quality indicating a low stored strain energy. In most cases, these Goss grains were found embedded in one of the two symmetrical $\{111\}\langle 112\rangle$ orientations. After the highest deformation degree of 89%, most of the remaining Goss-oriented crystal volume was surrounded by high-angle grain boundaries. The average diameter of the Goss residuals was about 0.3 μm .

In the less deformed material without shear bands the evolution of the initially Goss-oriented volume was clearly related to the development of microbands (Figs. 6,7 and 12). At some places the Goss-oriented regions were already completely surrounded by high-angle grain boundaries (Fig. 13). Other Goss-oriented regions partly showed

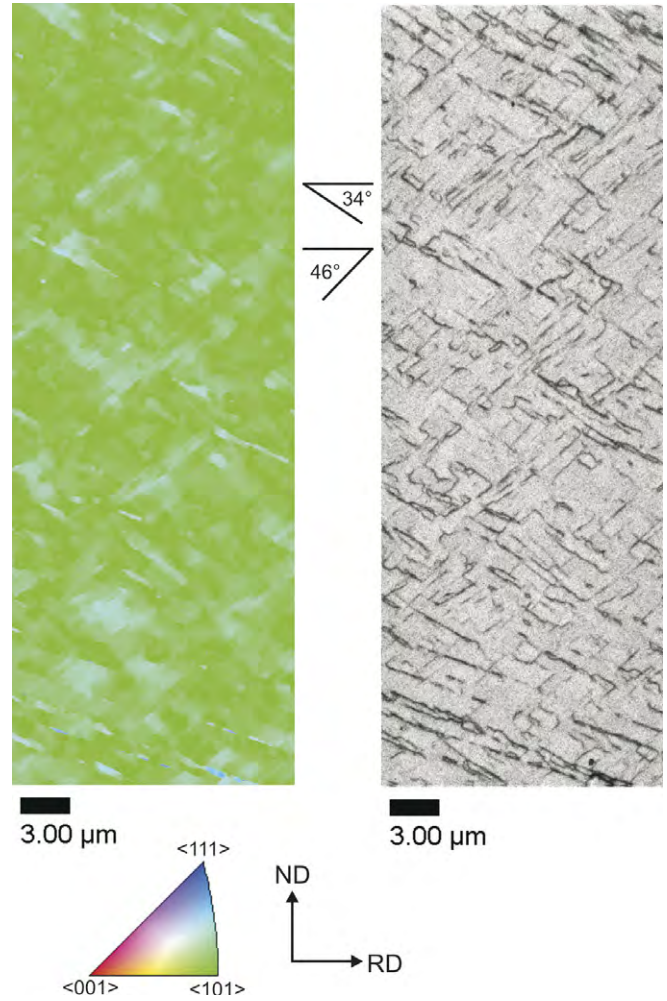
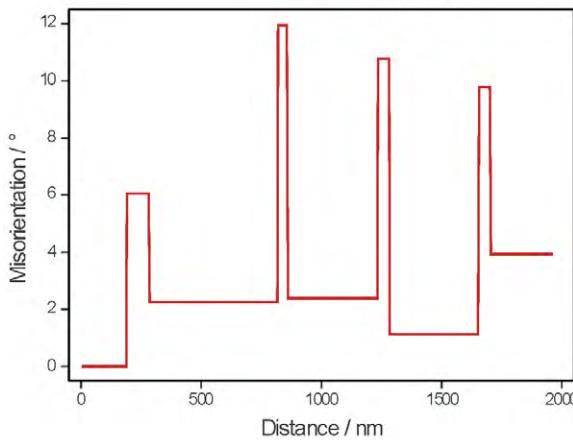
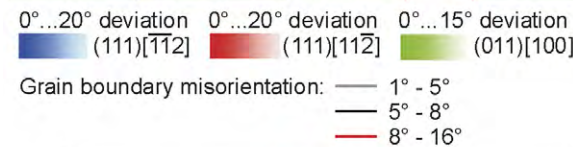
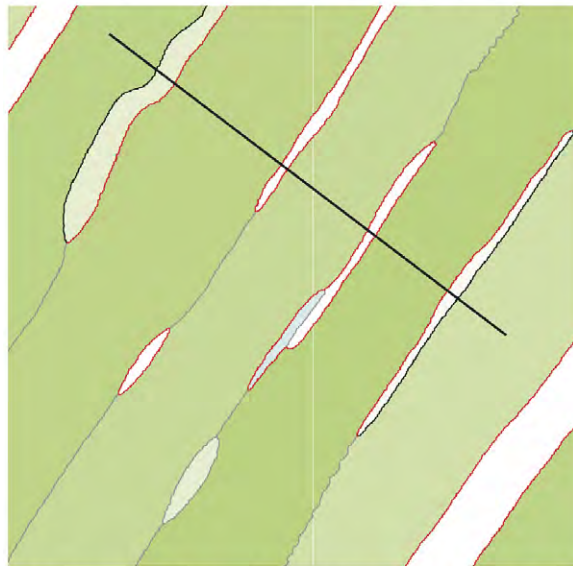
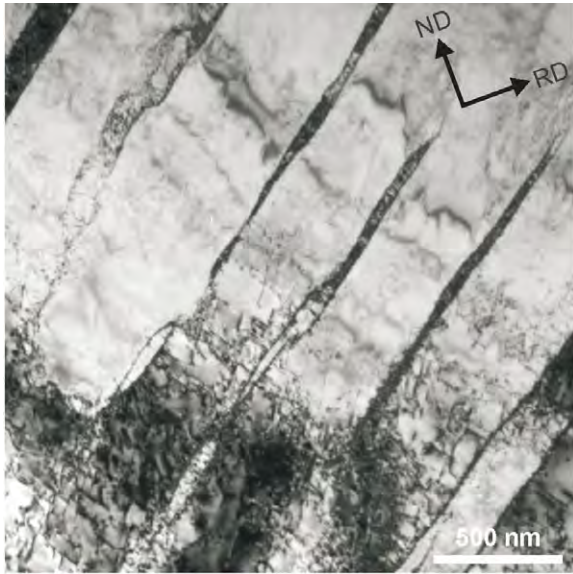


Fig. 8. 55% deformed, initially Goss-oriented FeSi single material with a region characterised by two crossing sets of linear microstructural features that are supposed to be early stages of microband evolution. (a) Inverse pole figure map for the normal sample direction as obtained by EBSD. (b) EBSD pattern quality map showing microbands as linear features with low EBSD pattern qualities.

high-angle grain boundaries and were partly in a continuous orientation gradient (Fig. 13). This indicated that the Goss grains between the microbands first form high-angle grain boundaries across the microbands, while parallel to the microbands the orientation continuously changed. Across the high-angle grain boundaries the orientation difference frequently approached 35°, which is the misorientation between the Goss and the two {111}<112> orientations. TEM investigations showed that the high-angle grain boundaries of the Goss grains are very sharp (Fig. 14).

Fig. 7. Microbands with open and closed parts in a 55% deformed initially Goss-oriented FeSi single crystal. (a) TEM bright field image. (b) Crystal orientation map. (c) Misorientation profile along the line in (b).

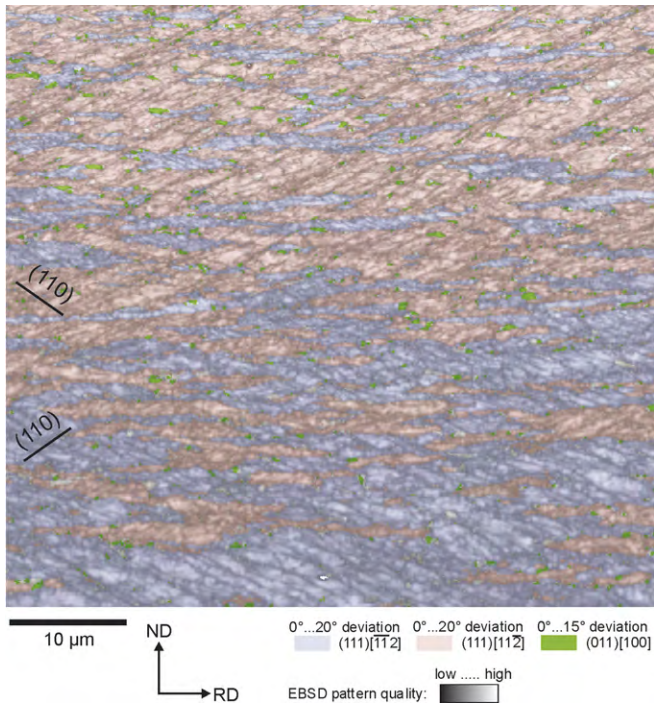


Fig. 9. Correlation of the inclination direction of shear bands with the particular $\{111\}\langle 112\rangle$ orientation in the 89% deformed material. The orientations of the $\{110\}$ planes are indicated (see also Fig. 16). EBSD pattern quality map combined with the corresponding crystal orientation. Shear bands are visible as linear features with a low EBSD pattern quality.

4. Discussion

4.1. Stability of the Goss orientation during cold rolling

Taylor-type as well as corresponding crystal-plasticity finite element simulations showed that bcc crystals with

Goss orientation are unstable under plane strain deformation [12,13]. More precisely, while the mathematically *exact* $\{110\}\langle 001\rangle$ orientation is stable under ideal plane strain loading, very small deviations from the exact Goss orientation or slight changes in the boundary conditions, e.g. friction, lead to a transverse rotation towards the two symmetrical $\{111\}\langle 112\rangle$ orientations [18,12]. In contrast, under pure shear strain deformation, the $\{111\}\langle 112\rangle$ orientations rotate into the Goss orientation, which is stable in this case [12,18]. In general, cold rolling can be approximated as a plane strain deformation state, if shear strain due to friction at the sheet surface is negligible. Therefore, in this study, the initial Goss orientation should be unstable during cold rolling. Indeed, this was observed for the major volume fraction of the cold rolled silicon steel sheet (Figs. 3 and 9–11). However, about 2.0–2.5% of the material formed small islands with Goss orientation (considering a misorientation up to 15°) even after as much as 89% thickness reduction of an initially Goss-oriented single crystal (Figs. 9–11).

In the following sections the origin of the remaining Goss-oriented crystal volumes is discussed with respect to two conceivable mechanisms corresponding to the two types of observed Goss regions. First, the generation of the Goss orientation in shear bands is presented. Second, we discuss the retention of small Goss-oriented crystal volumes between microbands.

4.2. Formation of Goss grains inside of shear bands

The role of shear bands in the context of the Goss texture formation in silicon steel has already been investigated by Haratani et al. [19] and Ushioda and Hutchinson [20]. However, they could not resolve the microstructure of the shear bands in the cold rolled state. In this study, it

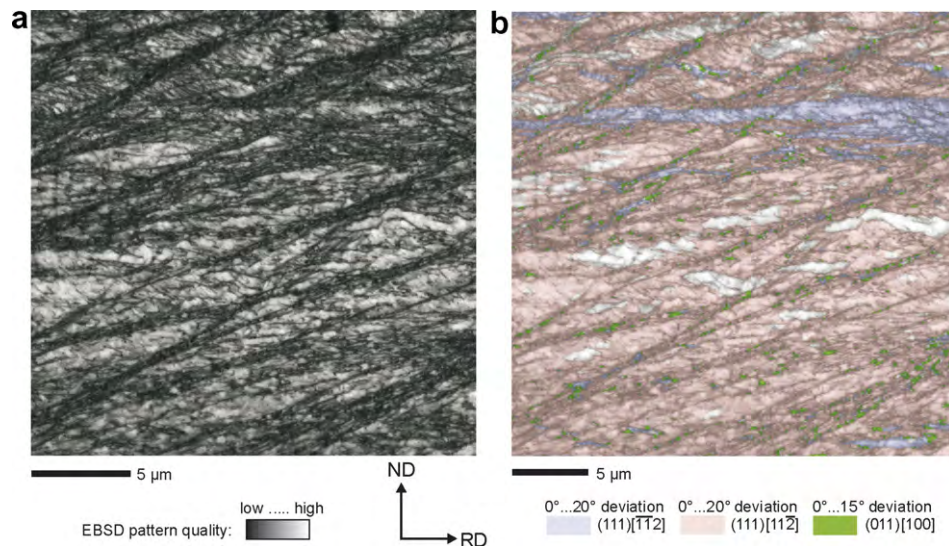


Fig. 10. Goss grains inside of shear bands in the 89% deformed material. (a) EBSD pattern quality map showing shear bands as regions with low EBSD pattern qualities. (b) Same map as in (a) combined with the corresponding crystal orientation. The Goss-oriented regions are aligned along the shear bands.

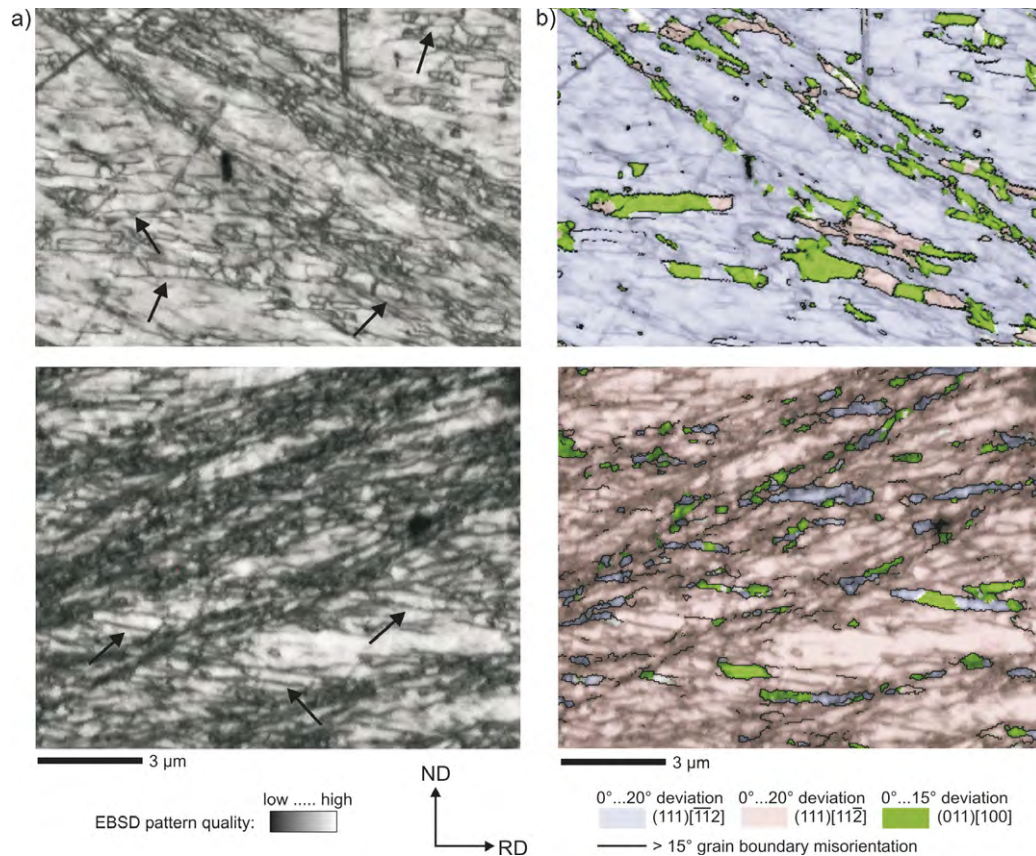


Fig. 11. Goss grains between microbands in the 89% deformed material. (a) EBSD pattern quality map showing parallel microbands as parallel linear features with low pattern quality (see arrows). In addition, shear bands are present. (b) Same map as in (a) combined with the corresponding crystal orientation. Goss grains that are aligned inside of shear bands are also visible.

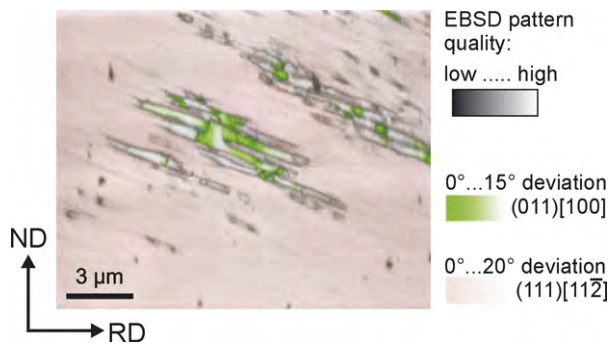


Fig. 12. Relation of microbands and Goss-oriented crystal volumes. 55% deformed material. EBSD pattern quality map combined with the corresponding crystal orientation.

was observed that a part of the Goss grains that were found after high strain was aligned inside shear bands. This observation, and the fact that shear bands started to form only after a strain of about 77% thickness reduction, indicated that the Goss orientation formed due to the local shear deformation in the shear bands. Therefore, it was assumed that, at first, the initial Goss orientation rotates to the two $\{111\}\langle 112 \rangle$ orientations. At higher deformation degrees, when the shear bands are formed, the $\{111\}\langle 112 \rangle$ orienta-

tions then rotate back to the Goss orientation due to the local shear strain in the shear bands. In this context, the question arose why only part of the material within the shear bands rotated back to the Goss orientation while the rest remained in the $\{111\}\langle 112 \rangle$ orientations [16]. The alternative possibility that the initial Goss orientation was retained within the shear bands could be excluded because shear bands first formed at a strain when most of the Goss orientation had already rotated into the $\{111\}\langle 112 \rangle$ orientations.

4.3. Development of microbands and retention of the Goss orientation between microbands

Goss grains, which are surrounded by high-angle grain boundaries, were found between microbands in the highest deformed material (Figs. 11 and 14). In earlier deformation stages, Goss-oriented regions were also observed between microbands (Figs. 6, 7, 12 and 13). These observations indicated that the retention of the initial Goss orientation and the development of microbands are closely related. In the following it is outlined how the microbands develop, and a tentative explanation is given that describes how the Goss orientation might be retained between the microbands.

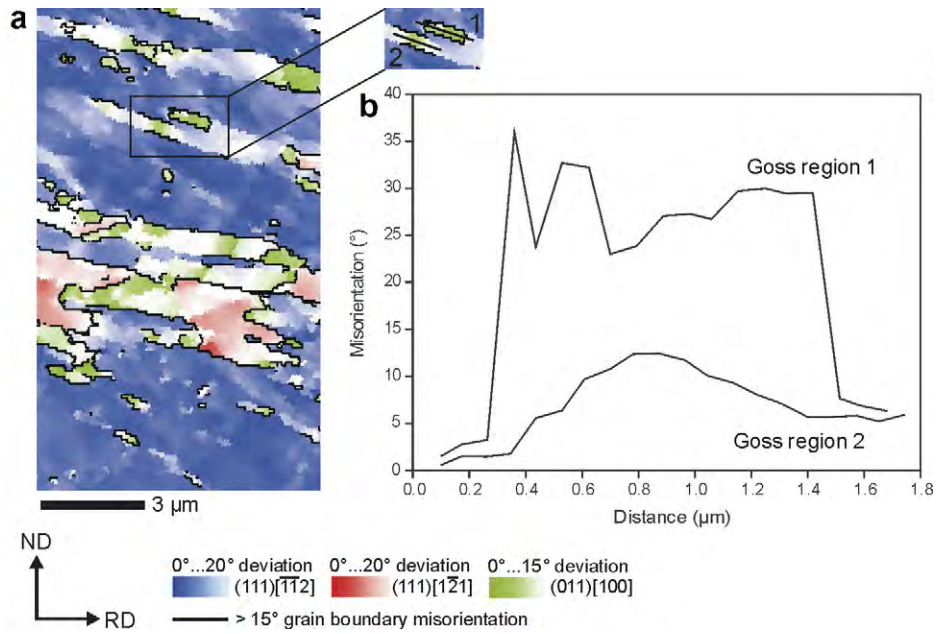


Fig. 13. (a) Goss-oriented regions in the 70% deformed material. (b) Misorientation profiles for Goss region 1, which is completely surrounded by high-angle grain boundaries, and for Goss region 2, which forms an orientation gradient with the {111}⟨112⟩ matrix.

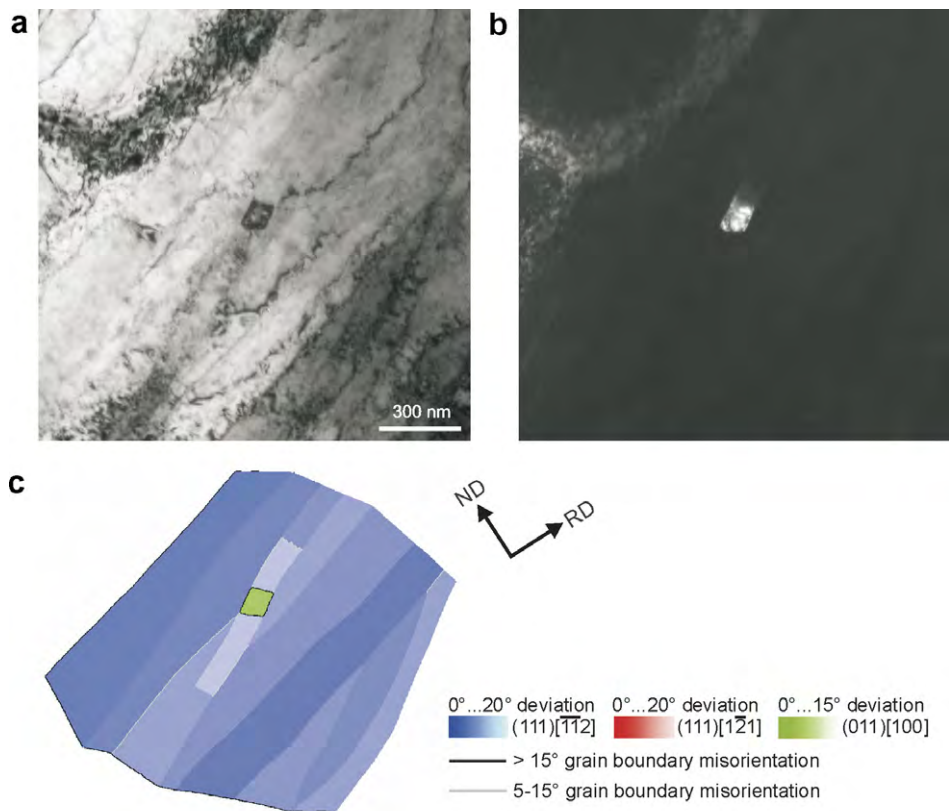


Fig. 14. Goss grain surrounded by sharp high-angle grain boundaries in the 66% deformed material. (a) TEM bright field image. (b) TEM dark field image. (c) Crystal orientation map for the same area as in (a) and (b). High-angle grain boundaries are marked in black, low-angle grain boundaries in grey.

In a first step, a fully constrained Taylor model was used in order to estimate which slip systems are active during the transverse lattice rotation from the {110}⟨001⟩ towards

the two {111}⟨112⟩ crystal orientations. The 12 {110}⟨111⟩ and the 12 {112}⟨111⟩ slip systems were taken into account for the determination of the Taylor factor, the

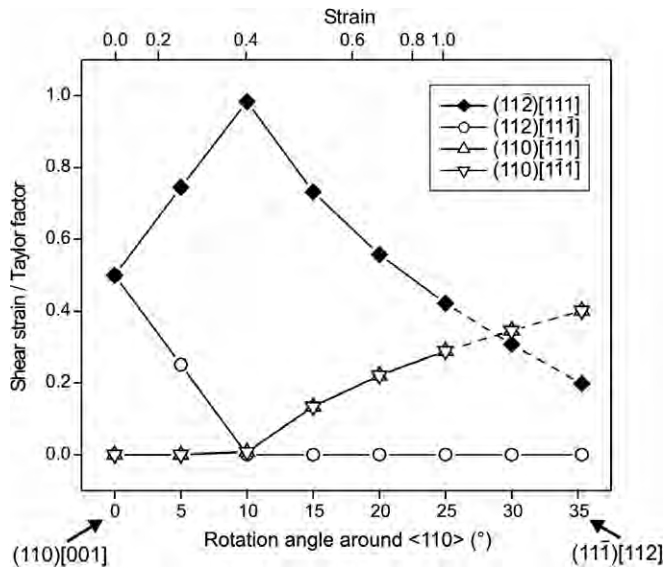


Fig. 15. Shear strain on different slip systems normalized by the Taylor factor as a function of rotation from $(110)[001]$ to $(11\bar{1})[112]$ around the $\langle 110 \rangle$ crystal direction. Strains corresponding to the lattice rotation are indicated at the upper axis. A fully constraint Taylor model with 24 slip systems for a bcc crystal was used to calculate the active slip systems.

active slip systems and the corresponding shear strain for each slip system. The main finding of the Taylor-type calculations was that the gradual orientation change from the Goss orientation to a $\{111\}\langle 112 \rangle$ crystal orientation is characterised by, first, a concentration of the dislocation activity on only one particular glide system for small rotation angles, and second, by a discontinuous transition of the second and third active slip systems with further increase of rotation and accordingly deformation (Fig. 15). Note that the fully constrained Taylor model gives the $\{11118\}\langle 4411 \rangle$ orientation as the stable end orientation for the Goss orientation. Therefore, in Fig. 15 the strains that correspond to the lattice rotation were only given for a rotation of up to 25° . In contrast to the simulations, the experimental results showed that for larger strains the lattice rotation continues towards the $\{111\}\langle 112 \rangle$ orientations (Fig. 3).

The microstructure observations, combined with the results obtained from the Taylor-type calculation on the active slip systems, yielded the following ideas on the activity of glide planes and shear bands and on microband development during the rolling process (Figs. 15 and 16). In the initial Goss orientation, slip starts on the two $\{112\}$ planes that are inclined by 55° to the rolling direction (Figs. 15 and 16a). In Fig. 8 crossing linear structures (resp. early microbands) possibly reflect this initial activity on two $\{112\}$ planes after some rotation had already occurred since the observed inclination is smaller than the theoretical 55° . During further rotation, the activity on one of these glide planes ceases, while activity on the other glide plane that rotates toward smaller inclination angles increases (Figs. 15 and 16b). The continuing activity

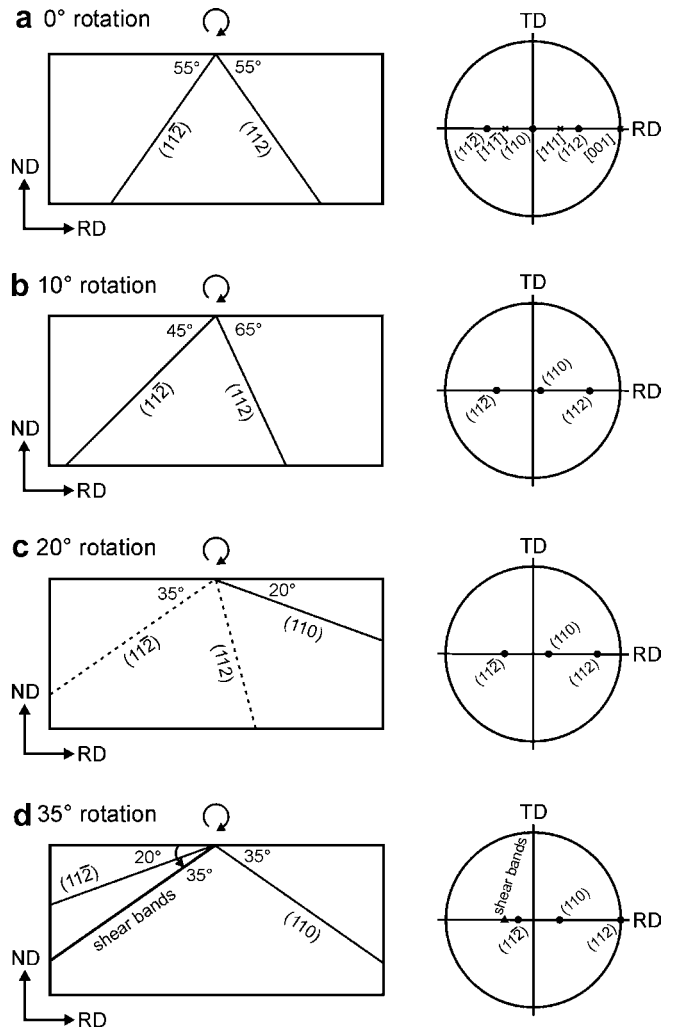


Fig. 16. Activity of glide planes and shear bands for four different rotation angles from $(110)[001]$ to $(11\bar{1})[112]$ around the $\langle 110 \rangle$ crystal direction.

on, in this example, $(11\bar{2})[111]$ (Figs. 15 and 16a–c) causes the formation of parallel microbands (Figs. 5 and 6). The significance of $\{112\}$ glide planes for the formation of microbands is confirmed by the observation that the microband habit plane is close to $\{112\}$, with a small deviation possibly due to some amount of pencil glide. According to Chen et al. [15], one set of microbands forms when the habit plane of the observed microband has the largest Schmid factor and when one $\langle 111 \rangle$ slip direction is intensively activated in this plane. This is valid for a Goss-oriented single crystal. For more than 10° of rotation, the activity on $(11\bar{2})$ decreases, while that on the (110) glide plane increases (Figs. 15 and 16c). After the full 35° rotation from Goss to $\{111\}\langle 112 \rangle$, the main slip activity is now on the (110) plane and therefore microband formation is assumed to have terminated. At this stage, shear bands form symmetrically to the (110) plane that is inclined by 35° to the rolling direction (Fig. 16d). This scenario is accordingly valid for the rotation of the Goss orientation to the other $\{111\}\langle 112 \rangle$ crystal orientation.

Dillamore et al. [21] explained the retention of the initial crystal orientation by a transition band model. Their idea is that an unstable starting orientation rotates toward symmetrical orientations in two directions and the initial orientation is retained in a transition band between the stable end orientations. In the present study, this would correspond to a situation where the initial Goss orientation persists in a transition band between the two symmetrical $\{111\}\langle 112 \rangle$ orientations. However, we found that the Goss regions that were retained between microbands were mostly situated in one $\{111\}\langle 112 \rangle$ orientation, not between the two different $\{111\}\langle 112 \rangle$ components. Thus, the Dillamore transition band model does not explain the observed retention of the Goss orientation between microbands. Therefore, we suggest the following tentative explanation for the Goss retention, which is based on the idea that in a small crystal volume a different set of slip systems is active compared with in the surrounding material. While experimentally the Goss orientation is unstable under plane strain loading conditions, the mathematically exact Goss orientation under exact plane strain loading conditions does not rotate, because the opposite rotations towards the two symmetrical $\{111\}\langle 112 \rangle$ orientations exactly compensate. However, even a slight deviation from exact Goss or a slight deviation from the exact plane strain condition, e.g. due to local stress heterogeneities, favours one of the sets of slip systems and causes a rotation of the Goss orientation towards one of the stable end positions. On the macroscopic scale, depending on the macroscopic stress conditions, parts of the originally Goss-oriented crystal rotate in one direction while other parts rotate in the other direction towards $\{111\}\langle 112 \rangle$. Locally, however, stress heterogeneities, e.g. due to microbands that act as dislocation obstacles, might activate that set of slip systems that causes lattice rotation into the opposite direction. This leads to the situation displayed in Fig. 17: a small crystal volume, in which different slip systems are active compared with in the surrounding material, might be temporarily considered as a rigid inclusion (Fig. 17a). The surrounding matrix rotates in one direction, thereby imposing a similar rotation on the inclusion in the form of a rigid body rotation (Fig. 17b). Inside this so-called inclusion, a different, but symmetrical set of slip systems causes the exact opposite lattice rotation, thus balancing out the externally imposed rotation (Fig. 17c). This leads to a zero net rotation, and thus the initial Goss orientation is retained in that small crystal volume. This process is, however, quite critical as the internal rotation in the small regions must always be slightly ahead of the macroscopic external rotation. Otherwise the set of slip systems that causes lattice rotation in the same sense as the matrix would be activated and the Goss orientation would no longer be stable, but would rotate in the same direction as the matrix. In fact, the experimental data for low rolling degrees show that there are more Goss-oriented regions between microbands in the less strained material (Fig. 6). In some places the retained Goss areas are embedded in a matrix of one of

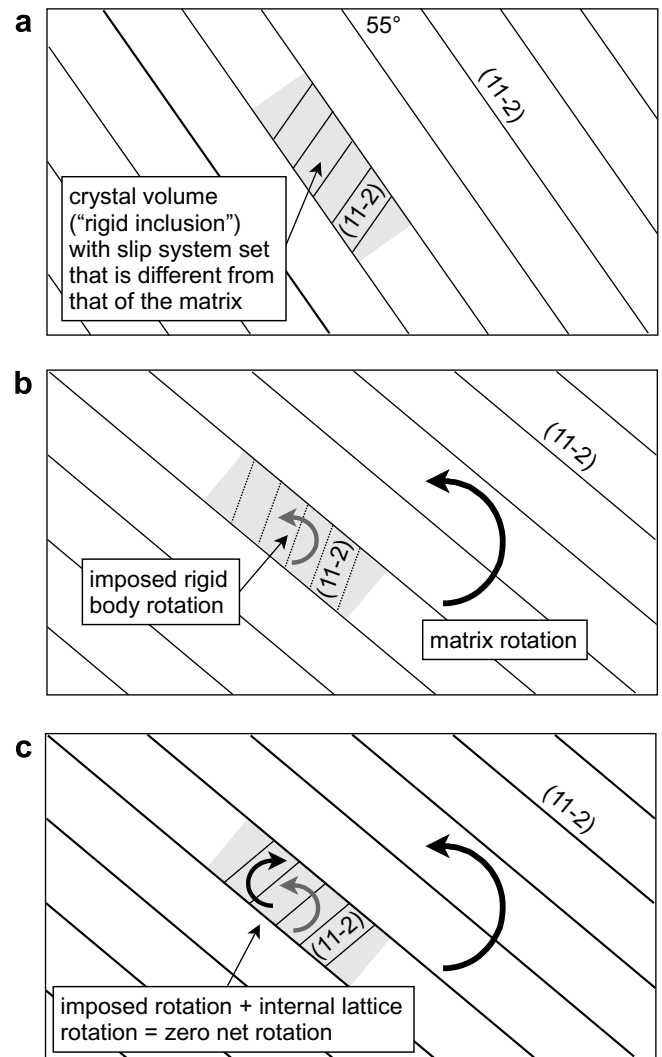


Fig. 17. Tentative idea for the retention of Goss-oriented crystal volumes between microbands. The mechanism is based on the idea that in a small crystal volume an internal lattice rotation and an externally imposed rigid body rotation compensate each other, resulting in zero net rotation. For a detailed description see the text.

the $\{111\}\langle 112 \rangle$ components, but small areas of the other $\{111\}\langle 112 \rangle$ components can be found on both ends. This observation supports the idea of a different set of slip systems being active in small areas between microbands, causing correspondingly different lattice rotations. The reason for different deformation characteristics in small, confined areas might be local stress heterogeneities. However, more work is required to understand the details of this process.

Concluding, we suppose that the origin of Goss-oriented regions between microbands is the initial Goss orientation of the single crystal that is retained in small crystal volumes. This is in contrast to the origin of the Goss-oriented regions inside shear bands that rotate back to the Goss orientation after a change in the deformation mode from plain strain to shear.

5. Summary and conclusions

An initially Goss-oriented FeSi single crystal was cold rolled to a thickness reduction of 89%. In the course of rolling, most of the material rotated into the two symmetrically equivalent $\{111\}\langle 112 \rangle$ orientations. However, a weak Goss texture component was observed in the highly deformed material, even though the Goss orientation is not stable under plane strain deformation. Investigation of the deformed microstructure led to the identification of two types of Goss-oriented regions with different origins. One type was found in highly strained material inside shear bands. These Goss regions formed in the shear bands that developed at thickness reductions of more than 70%. The second type of Goss regions was situated between microbands, i.e. in regions with low stored strain energy. The origin of the Goss orientation between the microbands is the initial Goss orientation. A tentative explanation outlines how these Goss-oriented regions were retained from the initial Goss orientation of the single crystal. It is proposed that in small areas between microbands a different set of slip systems is active compared with in the surrounding material. Under favourable conditions the rotation in this area compensates the opposite rigid body rotation imposed by the surrounding material and the initial Goss orientation is retained.

The sharp Goss orientation that develops during secondary recrystallisation in industrially processed silicon steel has its origin in the hot rolling stage. In this study, two types of Goss regions were observed after cold rolling of an initially Goss-oriented single crystal. Provided that the results on single crystals can be transferred to polycrystalline material, it might be concluded that the Goss-oriented regions that are found between microbands and that are assumed to be stable during cold rolling have special significance for the formation of Goss grains in the primary recrystallised material, and, consequently, for the

abnormal growth of Goss grains during secondary recrystallisation. If the newly formed Goss grains inside the shear bands were specifically relevant, then the removal of the surface layer would not change the formation of Goss grains during primary recrystallisation [5,1,6].

Acknowledgement

The authors gratefully acknowledge financial support by ThyssenKrupp Electrical Steel GmbH. The same company also kindly provided the sample material for this research project.

References

- [1] Mishra S, Därmann C, Lücke K. *Acta Metall* 1984;32:2185.
- [2] Matsuo M, Sakai T, Yozo S. *Metall Trans* 1986;17A:1313.
- [3] Shimizu Y, Ito Y, Iida Y. *Metall Trans* 1986;17A:1323.
- [4] Matsuo M. *ISIJ Int* 1989;29:809.
- [5] Böttcher A, Lücke K. *Acta Metall Mater* 1993;41:2503.
- [6] Pease NC, Jones DW, Wise MHL, Hutchinson WB. *Met Sci* 1981;15:203.
- [7] Dorner D, Zaefferer S, Lahn L, Raabe D. *J Magn Magn Mater* 2006;304:183.
- [8] May JE, Turnbull D. *Trans Metall Soc AIME* 1958;212:769.
- [9] Seidel L, Hölscher M, Lücke K. *Texture Microstruct* 1989;11:171.
- [10] Zaefferer S, Chen N. *Solid State Phenom* 2005;105:29.
- [11] Dunn CG. *Acta Metall* 1954;2:173.
- [12] Raabe D, Zhao Z, Park S-J, Roters F. *Acta Mater* 2002;50:421.
- [13] Hölscher M, Raabe D, Lücke K. *Steel Res* 1991;62:567.
- [14] Zaefferer S. *J Appl Cryst* 2000;33:10.
- [15] Chen QZ, Ngan AHW, Duggan BJ. *Proc R Soc London A* 2003;459:1661.
- [16] Dorner D, Zaefferer S. *Solid State Phenom* 2005;105:239.
- [17] Dillamore IL, Roberts JG, Bush AC. *Met Sci* 1979;13:73.
- [18] Hölscher M, Raabe D, Lücke K. *Acta Metall Mater* 1994;42:879.
- [19] Haratani T, Hutchinson WB, Dillamore IL, Bate P. *Met Sci* 1984;18:57.
- [20] Ushioda K, Hutchinson WB. *ISIJ Int* 1989;29:862.
- [21] Dillamore IL, Morris PL, Smith CJE, Hutchinson WB. *Proc R Soc London A* 1972;329:405.